SH-Containing Cellulose Acetate Derivatives: Preparation and Characterization as a Shape Memory-Recovery Material

Dan Aoki, Yoshikuni Teramoto,† and Yoshiyuki Nishio*

Division of Forest and Biomaterials Science, Graduate School of Agriculture, Kyoto University, Sakyo-ku, Kyoto 606-8502, Japan

Received June 20, 2007; Revised Manuscript Received September 13, 2007

Cellulose derivatives having a cross-linkable mercapto group were prepared by esterification of cellulose acetate (CA) with mercaptoacetic acid. The molecular structure of a series of products (CA-MA) was characterized by ^{1}H and ^{1}H-^{13}C HMQC NMR spectroscopy and gel permeation chromatography. The solubility of CA-MA in water and organic solvents could be controlled by changing the preparation conditions including the degree of acetyl substitution of the starting CA. The CA-MA samples thus synthesized showed a sol–gel transition in solution and a shape memory-recovery behavior in film form through adequate redox treatments due to the reversible, cross-linking association and dissociation between mercapto groups. Dimethyl sulfoxide was usable as the organic solvent and oxidant, while the major reducing reagent was 2-mercaptoethanol or ammonium mercaptoacetic acid. The progress of the redox reactions was followed by using a confocal depth scanning technique in Raman spectroscopy. It was found that the compatibility between the cellulose derivatives and the redox reagents used was an important factor for the successful reactions, especially in the samples of film form. The cross-linking effect on the thermal and viscoelastic properties of the CA-MA films was also estimated by differential scanning calorimetry and dynamic mechanical analysis. Discussion focused on the alternately declining and recovering behavior of a principal loss tan δ peak, observed following the redox treatments repeated for the CA-MA film specimens.

Introduction

Cellulose has been used from ancient times as an important polymeric material in the fields of shelter, clothing, and paper. In recent years, there have been significant advances in novel designing of functionalized cellulose derivatives.[1,2] The elaborate chemical modifications should cultivate further applications of cellulosics.

Among many derivatizations of cellulose, there have been some attempts to incorporate a cross-linkable mercapto group (SH) into the molecular structure. For example, several works were conducted for the purpose of applying such SH-containing cellulose derivatives as a precursor for graft copolymerization,[3] an immobilizer for enzymes,[4] a thin coating on metal surfaces,[5] and adsorbents for metal ions[6] and the so-called Ellman's reagent.[7] An amino polysaccharide chitosan has also been modified with mercapto groups to prepare a cross-linked gel applicable to the drug delivery system.[8] In addition, there have been practically important studies on the introduction of disulfide cross-links into cotton fibers in relation to improvements of the mechanical property and the stability in figure of the textile products.[9–12] However, we find very few investigations[11,12] dealing with SH-containing polysaccharides for functionalization making full use of the "reversibility" of the cross-linking reaction.

The present study is concerned with preparation of cellulose acetate (CA) derivatives in which some of the residual hydroxyls of the starting CA are replaced by a short chain with a mercapto group at the terminal. CA is an industrially important cellulose ester, widely usable due to desirable physical properties involving good optical clarity in film form and a comparatively high modulus and adequate flexural and tensile strengths in fiber form. In addition, CA has been reported to be practically biodegradable.[13,14] If this cellulose derivative is invested with the cross-linking functionality, the practical availability will be more expanded in different material forms whether the target system is a solution or solid.

In this paper, first, conditions for preparing the CA derivatives having mercapto groups, termed CA-MA, with mercaptoacetic acid in a homogeneous solution system is described in detail. The main objective of the present study is to demonstrate a shape memory-recovery behavior of CA-MA following on–off switching of the cross-linkage of mercapto groups, both in solution and in film form. Redox reactions responsible for the reversible effect are analyzed for the film samples by depth scanning Raman spectroscopy. The redox-treated samples are also characterized by dynamic mechanical analysis for a possible change in the viscoelastic property.

Experimental Section

Materials. Three cellulose acetate (CA) samples were kindly supplied by Daicel Chemical Industries, Ltd. (Himeji, Japan). Values of the degree of acetyl substitution (DS_{Ac}) of the respective CAs, determined by ^{1}H NMR measurements (see below), were 2.18, 2.48, and 2.95. Mercaptoacetic acid (MAA) was purchased from Nacalai Tesque Inc. and distilled before use. 1,3-Dimethyl-2-imidazolidinone (DMI) and pyridine were purchased from Nacalai Tesque Inc. and stored over molecular sieves 4A before use. Propionic anhydride, 4-(dimethylamino)pyridine, dimethyl sulfoxide (DMSO), 2-mercaptoethanol (ME), 50 wt % ammonium mercaptoacetic acid aqueous solution (50% AMaq), and other reagents were purchased from Wako Pure Chemical Industries Ltd. and used as received. O_2 gas, 95%, was

* To whom correspondence should be addressed. E-mail: ynishio@kais.kyoto-u.ac.jp. Tel.: +81 75 753 6250. Fax: +81 75 753 6300

† Present address: Biomass Technology Research Center, National Institute of Advanced Industrial Science and Technology, 2-2-2 Hirosuehiro, Kure, Hiroshima 737-0197, Japan.

10.1021/bm7006828 CCC: $37.00
Published on Web 11/22/2007

purchased from PIP-Fujimoto Co. Ltd. and used as received. Distilled water was deaerated under reduced pressure and bubbled with N_2 gas before use.

Synthesis of CA-MA. CA (5.0 g, DS_{Ac} = 2.18 or 2.48) was added to 50 g of DMI and the mixture was stirred for 12 h at 20 °C. The resulting homogeneous solution was heated at 110 °C in an oil bath with stirring under a nitrogen atmosphere. MAA (12–24 eq/anhydroglucose residue of CA) was dropped into the hot solution. After a prescribed time period (0.5–24 h), the homogeneous solution was reprecipitated in an excess amount of methanol. The product, cellulose acetate mercaptoacetate (CA-MA), was purified by dissolving in tetrahydrofuran (THF) and reprecipitating into methanol and then filtering. Subsequently, the product was dried at 40 °C for 48 h in a vacuum oven.

Preparation of Water-Soluble Cellulose Acetate. To prepare water-soluble CA (wCA), deacetylation of cellulose triacetate was carried out by modifying an acid hydrolysis method that was formerly proposed by Miyamoto et al.[15] as follows. Ten g cellulose triacetate (DS_{Ac} = 2.95) was added to 100 mL of dichloromethane with stirring. After a homogeneous solution was obtained, 100 mL of acetic acid was added into the dichloromethane solution under stirring, followed by removing dichloromethane under reduced pressure at 40 °C, whereupon a clear acetic acid solution of cellulose triacetate was obtained. Subsequently, 100 mL of a mixture of acetic acid and water (4:1 in volume) was added dropwise into the solution under stirring at 40 °C. The deacetylation reaction of cellulose triacetate started with further addition of sulfuric acid (0.8 mL) as a catalyst. Then 40, 24, and 40 mL of H_2O were dropped into the solution after the passage of 16, 40, and 52 h, respectively. After 213 h elapsed in the total time, the homogeneous mixture was reprecipitated in an excess amount of acetone. The resulting wCA was dissolved in water, reprecipitated into acetone, and filtered after washing with methanol. Finally, the product was dried at 40 °C for 48 h in a vacuum oven.

Synthesis of wCA-MA. wCA (1.0 g, DS_{Ac} = 0.75) was added to 50 g of DMI, and the mixture was stirred for two weeks at 20 °C. The resulting homogeneous solution was heated at 110 °C in an oil bath with stirring under a nitrogen atmosphere. MAA (18 eq/anhydroglucose residue of wCA) was dropped into the hot solution. After 8 h, the homogeneous mixture was reprecipitated in an excess amount of methanol. The product, water-soluble cellulose acetate mercaptoacetate (wCA-MA), was purified by dissolving in water, reprecipitating into THF, and washing with methanol. Then, the purified wCA-MA was dried at 40 °C for 48 h in a vacuum oven.

Propionylation of Cellulose Derivatives. Propionylation of cellulose derivatives was conducted according to a method proposed by Tezuka et al.[16] The propionylation method is often used for characterization of cellulose ester derivatives because it improves the resolution of chemical shift in NMR spectra and seldom decreases the original acyl DS of the derivatives.[16,17]

Cellulose derivative (0.1 g) and 0.05 g of 4-(dimethylamino)pyridine were added to 5 mL of pyridine, and the mixture was stirred for 10 min at 20 °C. The resulting solution was heated at 100 °C, and 1.5 mL of propionic anhydride was dropped into it. After 100 min, the solution was reprecipitated in an excess amount of methanol. Propionylated CA (p-CA), propionylated wCA (p-wCA), propionylated CA-MA (p-CA-MA), and propionylated wCA-MA (p-wCA-MA) thus obtained were purified by dissolving in dichloromethane and reprecipitating into methanol. The purified products were dried at 40 °C for 48 h in a vacuum oven. In the modification of wCA and wCA-MA bearing many unsubstituted hydroxyl groups, however, the reaction time was prolonged to 200 min to accomplish the thorough propionylation, essential for determination of DS.

Redox Treatments of CA-MA and wCA-MA. Redox treatments of the mercaptoacetylated derivatives of CA were carried out in the solution state (for CA-MA and wCA-MA) and in the solid state of a film form (for CA-MA). DMSO, 20 wt % aqueous solution of DMSO (20% DMSOaq), or O_2 gas was used for the oxidation, while the reductants applied included ME, 10 wt % aqueous solution of ME (10% MEaq), a mixture of ME:DMI = 50:50 in weight (50% ME/DMI), 50% AMaq, 10 wt % aqueous solution of AM (10% AMaq), and a mixture of AM:DMI:H_2O = 10:10:80 in weight (10% AM/DMIaq). Abbreviations specifying the major reagents and polymer samples used are listed in the end of the text.

In a solution experiment, 0.2 g of CA-MA was dissolved in 6.4 g of DMSO at 20 °C. After the rapid dissolution, the solution became gelatinous gradually with time at the temperature and, ultimately, completely gelated usually in 24 h, following the progressive formation of cross-links between CA-MA chains owing to a thiol-oxidizing ability of DMSO[18] (see later discussion). To reduce the gel, in turn, 2.0 g of 50% AMaq was pored over the mixture; this reducing agent is commonly used for permanent wave treatment of hairs. After 1 h, the resultant solution (actually, incompletely reduced sol) was reprecipitated in an excess amount of methanol. The precipitate was washed with methanol, filtered, and dried at 40 °C for 24 h in vacuo. Subsequently, the sample was dissolved in 4.0 g of 50% ME/DMI at 20 °C and reduced thoroughly in the absence of DMSO. After stirring for 48 h, the homogeneous solution was reprecipitated in an excess amount of methanol, and the precipitate was filtered and washed with methanol, then dried at 40 °C for 48 h in a vacuum oven.

In another redox experiment in solution, an aqueous solution was prepared by dissolving 0.4 g wCA-MA in 19.6 g distilled water. The oxidation was carried out with O_2 bubbling (100 mL min^{-1}) for 20 s, and the resulting gel was reduced with addition of 5.0 g of ME at 20 °C. After 24 h, the reduced solution was reprecipitated in an excess amount of THF. The product was filtered, washed with methanol, and dried at 40 °C for 48 h in a vacuum oven.

In solid-state experiments, optically clear films of CA-MA were prepared by casting from the solutions in THF. The thickness of the cast films was regulated to be ca. 120 μm for dynamic mechanical analysis (DMA), or less than 10 μm for shape memory-recovery examinations. For oxidation, the film samples were immersed in 20% DMSOaq at 60 °C for 24 h and then washed thoroughly with distilled water. For reduction, 10% MEaq, 10% AMaq, or 10% AM/DMIaq was used at 30 °C. The films once oxidized were immersed in a selected reducing agent for a designated time period and washed with distilled water. The reducing agent used was exchanged for the fresh one every 24 h. Before DMA and Raman spectroscopy measurements, the CA-MA samples were all dried at 60 °C for three days in a vacuum oven after washing with distilled water.

In what follows, the number of redox treatments is designated by abbreviated notations; e.g., **o1** denotes that the considered sample was oxidized once, and **o1r1** signifies that the sample was oxidized once and then reduced.

Measurements. ^{1}H NMR spectra (400 MHz) were measured to determine DS values for different cellulose ester derivatives by using a Bruker AVANCE 400 NMR apparatus. The measuring conditions were as follows: solvent, $CDCl_3$; solute concentration, 30 mg mL^{-1}; internal standard, tetramethylsilane (TMS); temperature, 20 °C; number of scan, 64; recycle time of pulse, 6.45 s. A ^{1}H-^{13}C heteronuclear multiple-quantum correlation (HMQC) spectrum was measured by using a Bruker ARX 500 NMR apparatus to precisely assign the chemical shifts of p-CA-MA. The measuring conditions were as follows: solvent, $CDCl_3$; solute concentration, 100 mg mL^{-1}; internal standard, TMS; temperature, 20 °C; number of scan, 32 (^{1}H), 10000 (^{13}C), and 96 (HMQC).

Gel permeation chromatography (GPC) was carried out with a Tosoh HLC-8220 GPC apparatus. The measuring conditions were as follows: column, two Tosoh TSK Super HZM-H columns connected with each other; flow rate, 0.25 mL min^{-1}; temperature, 40 °C; eluent, THF; standard, monodispersed polystyrene.

To evaluate the redox state of mercapto groups for CA-MA samples, Raman spectra were measured by using a Horiba LabRam-350V microscopic Raman spectroscopy apparatus. The measuring conditions were as follows: internal standard, β-(1,4) glycosidic linkage at 1092

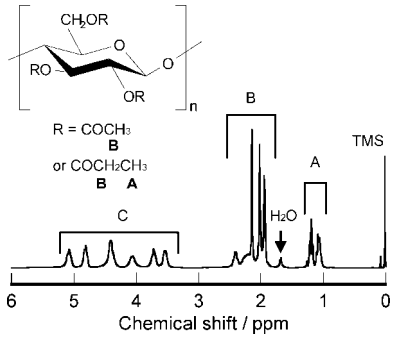

Figure 1. ^{1}H NMR spectrum of p-CA (DS_{Ac} = 2.18, DS_{Pr} = 0.90) in $CDCl_3$.

cm^{-1};[19–21] number of scans, 64; magnification, 50 times; numerical aperture, 0.80; spatial resolution of *X*-axis, 0.43 μm; spatial resolution of *Z*-axis, 1.20 μm. The *X*-axis lies in the surface plane of the film sample and the *Z*-axis is set in the depth direction perpendicular to the film surface. Raman spectra for powdered CA-MA samples collected after redox-treating in solution were measured with respect to the surface of the agglomerates. Spectra for CA-MA samples redox-treated in film form were measured at several selected positions different in depth from the film surface, usually at Z = 0, 10, 20, 40, and 60 μm.

Dynamic mechanical analysis (DMA) was conducted by using a Seiko DMS6100/EXSTAR6000 apparatus to evaluate a cross-linking effect on the viscoelastic property of CA-MA. Strips of rectangular shape (20 × 4 mm^2) cut from the solution-cast films ca. 120 μm thick were used for measurements of the temperature dependence of the dynamic storage modulus E' and mechanical loss tangent tan δ (= E''/E'; E'', loss modulus). The measuring conditions were as follows: temperature range, 20–270 °C; scanning rate, 2 °C min^{-1}; oscillatory frequency, 10 kHz. All the measurements were duplicated, and there was no substantial difference between the DMA data for two specimens prepared from the same film.

Differential scanning calorimetry (DSC) was carried out with a Seiko DSC6200/EXSTAR6000 apparatus. The temperature readings were calibrated with an indium standard. The measurements were made on ca. 4 mg samples packed in an aluminum pan, usually at a scanning rate of 20 °C min^{-1} under a nitrogen atmosphere. Preliminarily, each individual sample was heated from ambient temperature (25 °C) to 300 °C (first heating). Subsequently, a spare sample identical with the first one, packed in another aluminum pan, was heated from 25 to 230 °C and then immediately cooled to −50 °C at a rate of 80 °C min^{-1}. Following this, the second heating scan was run at 20 °C min^{-1} over the temperature range −50–300 °C (second heating). The glass transition temperature T_g, estimated in both first and second heating scans, was taken as a temperature at the midpoint of the discontinuity in heat flow.

Results and Discussion

NMR Characterization. DS values of CA, wCA, CA-MA, and wCA-MA were estimated by NMR spectroscopy. After propionylation, the cellulose derivatives were all soluble in $CDCl_3$, giving rise to well-resolved spectra.

^{1}H NMR spectra were obtained for propionylated CA (p-CA) and propionylated wCA (p-wCA). One of the data for p-CA (DS_{Ac} = 2.18, DS_{Pr} = 0.90) is shown in Figure 1, together with resonance-peak assignments. In the spectrum, we designate a resonance peak area derived from the methyl protons of propionyl groups as **A**; an overlapping peak area from the methyl protons of acetyl groups and the methylene protons of propionyl groups as **B**; and an area arising from the seven protons of the anhydroglucose residue as **C**. Then, the acetyl

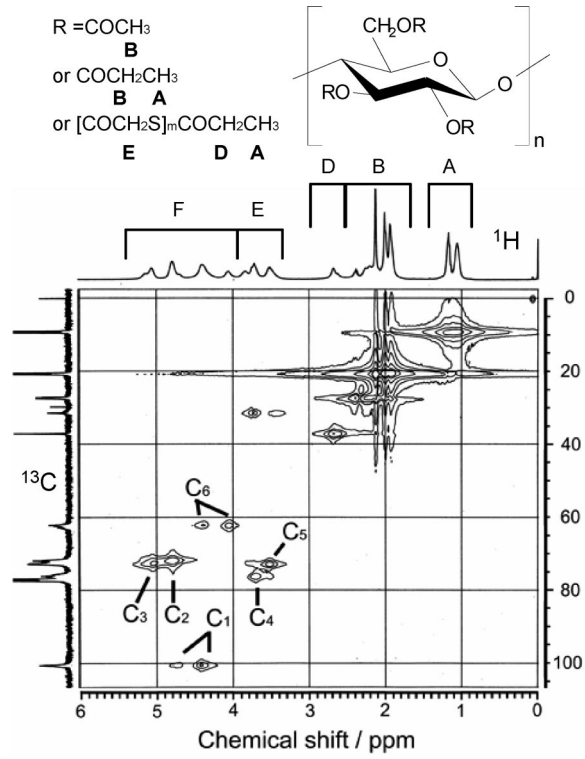

Figure 2. ^{1}H-^{13}C HMQC spectrum of p-CA-MA (DS_{Ac} = 1.80, DS_{SH} = 0.36, MS_{MA} = 0.43, DS_{Pr} = 1.33) in $CDCl_3$.

DS (DS_{Ac}) and propionyl DS (DS_{Pr}) can be evaluated by eqs (1) and (2), respectively.

$$DS_{Ac} = [(\mathbf{B} - 2\mathbf{A}/3)/3]/(\mathbf{C}/7) \quad (1)$$

$$DS_{Pr} = (\mathbf{A}/3)/(\mathbf{C}/7) \quad (2)$$

Figure 2 shows a ^{1}H-^{13}C HMQC spectrum of a propionylated CA-MA (p-CA-MA, DS_{Ac} = 1.80, DS of side chains having a mercapto terminal (DS_{SH}) = 0.36, molar substitution of mercaptoacetic acid (MS_{MA}) = 0.43, DS_{Pr} = 1.33), including peak assignments. All the proton signals of the anhydroglucose unit separated clearly. Possible substituents on p-CA-MA are simply considered to be acetyl, propionyl, and mercaptoacetyl groups. However, caution should be exercised to the possibility that MAA might have been polymerized by self-condensation because MAA has two reactive functional groups, namely carboxyl and mercapto groups (e.g., 2HS-CH_2-COOH → H[S-CH_2-$CO]_2$OH + H_2O). Therefore, it is natural to assume that the molar amount of the mercapto side-end groups present in CA-MA and the total molar amount of the introduced MAA are generally different from each other. Eventually, as for p-CA-MA, all protons and carbons of the anhydroglucose residue and of the actual substituents could be assigned as illustrated in Figure 2; here, the spectral data demonstrates that the mercapto groups were also thioesterified by propionic acid because the methylene peaks of propionyl groups emerged separately for the propionyl ester (OCO) and thioester (SCO) (peaks **B** and **D**, respectively). In consequence, we can quantify the amount of mercapto terminals of the side chains by reference to the peak area associated with the thioester.

As exemplified for the ^{1}H NMR spectrum in Figure 2, we designate an area of the resonance signal from the methylene protons of propionyl groups of the thioester as **D**; an overlapping peak area from the methylene protons of mercaptoacetyl groups and the C4— and C5— protons of the anhydroglucose residue as **E**; and an area from the other five protons of the anhydr

Table 1. DS Values of Starting Materials to be Modified with MAA, Estimated by ^{1}H NMR after Propionylation

sample code	DS_{Ac}	DS_{Pr}
CA 1	2.18	0.90
CA 2	2.48	0.57
wCA[a]	0.75	2.30

[a] Derived from cellulose triacetate whose DS_{Ac} and DS_{Pr} were evaluated as 2.95 and 0.11, respectively, after propionylation.

glucose residue as **F**, in addition to the previous definition of **A** and **B**. Then the values of DS_{Ac}, DS_{Pr}, and DS of side chains having a mercapto terminal (DS_{SH}) and that of the molar substitution of mercaptoacetic acid (MS_{MA}) are able to be determined by eqs (3–6), respectively.

$$DS_{Ac} = [(\mathbf{B} + \mathbf{D} - 2\mathbf{A}/3)/3]/(\mathbf{F}/5) \quad (3)$$

$$DS_{Pr} = (\mathbf{A}/3)/(\mathbf{F}/5) \quad (4)$$

$$DS_{SH} = (\mathbf{D}/2)/(\mathbf{F}/5) \quad (5)$$

$$MS_{MA} = [(\mathbf{E} - 2\mathbf{F}/5)/2]/(\mathbf{F}/5) \quad (6)$$

The result of the determination of substitution degrees is summarized in two tabulations: in Table 1, for the starting CA materials, and in Table 2, for CA-MA and wCA-MA samples, together with conditions of the mercaptoacetylating reactions. We find in both tables that the total DS ($= DS_{Ac} + DS_{Pr}$) of the respective propionylated samples was nearly 3.0.

In the preparation of CA-MA (Table 2), DS_{Ac} decreased with time of mercaptoacetylation, which can be interpreted as due to deacetylation and/or transesterification of the original acetyl groups by applying MAA. DS_{SH} linearly increased up to 0.59 with the time course of mercaptoacetylation of CA (in the case using CA 1), and MS_{MA} increased to an extent equal to DS_{SH} or exceeded this slightly. This implies that MAA hardly formed the thioester with itself under the reaction conditions adopted. As to wCA-MA, DS_{Ac} decreased to some extent by mercaptoacetylation of wCA, and DS_{SH} and MS_{MA} were found to be rather lower in comparison with the elevation in the values observed for CA-MA. To increase DS_{SH} of wCA-MA, an attempt was made to prolong the mercaptoacetylation time (8 h → 16 h); however, wCA-MA with a much higher, DS_{SH} was not obtained. Hereafter we designate CA-MA of $DS_{SH} = x$ as CA-MAx because DS_{SH} is an adequate parameter to indicate the redox activity discussed later.

Evaluation of Molecular Weight. Molecular weights of CA, wCA, CA-MA, and wCA-MA were evaluated by GPC after propionylation whereby the samples were easily dissolved in THF. Data of the number-average molecular weight (M_n), weight-average molecular weight (M_w), degree of polydispersity (M_w/M_n), and weight-average degree of polymerization (DP_w) of the derivatives are listed in Table 3. DP_w was estimated by division of M_w by a calculated molecular mass per repeating unit of the respective propionylated derivatives. From the result of the GPC analysis, it is found that the molecular weight of CA-MA decreased with mercaptoacetylation time, while no appreciable decrease in molecular weight was observed for wCA-MA. In the mercaptoacetylating reaction for wCA, the relative concentration of the solute in DMI was a fifth of that in the CA-MA synthesis. The lower-acetylated wCA would be solvated by DMI to a greater extent, than the situation of the higher-acetylated CA. This may be responsible for the observations for wCA-MA: the lower reactivity of the residual hydroxyls and the slower acid-hydrolysis of glycoside linkages in the cellulose backbone.

Raman Spectra of CA-MA. Figure 3 compiles Raman spectra (at $Z = 0$ μm) obtained for CA ($DS_{Ac} = 2.48$), as-prepared CA-$MA_{0.23}$, once oxidized CA-$MA_{0.23}$ (**o1**, 20% DMSOaq-treated), and oxidized and then reduced CA-$MA_{0.23}$ (**o1r1**, 10% MEaq-treated), all the samples being in film form. After oxidation, a peak intensity at 2575 cm^{-1} assigned to the mercapto group (I_{SH}) vanished and, at the same time, a peak intensity at 500 cm^{-1} assigned to the SS group (I_{SS}) increased, but not remarkably. After reduction of the oxidized sample, I_{SH} recovered and I_{SS} decreased. The spectrum of the as-prepared CA-$MA_{0.23}$ and that of **o1r1** are essentially indistinguishable from each other. This observation indicates that the CA-$MA_{0.23}$ contains almost no disulphide linkage just after production, which may be consistent with the report that MAA forms few disulphide bonds in an acidic condition.[8] Other CA-MAs also exhibited similar redox behavior, and the as-produced samples were all taken to be free of disulphide cross-linking.

The oxidation of CA-MA was also possible by the use of pyridine instead of DMSO (see below). In that case with pyridine, too, we obtained essentially the same Raman result as that mentioned above.

Sol–Gel Transition. As-prepared CA-MA samples showed a good solubility in pyridine and DMSO, but the solutions in these solvents gelated within a few days after dissolution due to the S–S cross-linking formation by virtue of the thiol oxidation ability of DMSO[18] and, as well, of the proton-accepting ability of basic pyridine. Figure 4 demonstrates an example of the visual appearance of the sol–gel transition for CA-$MA_{0.23}$.

When a reducing agent was added onto the oxidized CA-MA/solvent systems, the extent of gelation decreased gradually with time depending on the reductant species used. In the employment of ME, it took 48–96 h to completely solate the CA-MA gel. With 50% AMaq, 1 h was enough to solate the gel. Therefore, evidently AM has a reducing ability higher than that of ME. In the sol produced by using 50% AMaq, however, a white precipitation occurred in 2 days after reducing, while the sol reduced with ME was stable even after standing for a few months. This difference can be attributed to the difference in compatibility of CA-MA with the respective reducing agents. In fact, as-prepared CA-MAs were soluble directly in ME and, as well, in aqueous solutions containing more than 50 wt % ME, whereas they neither dissolved nor swelled in 50% AMaq. Thus, in spite of the stronger reducing power, AM is of less advantage to the effective reducing treatment due to the poor compatibility with CA-MA.

Effects of the DS_{SH} and molecular weight of CA-MA on the gelation behavior were visually investigated systematically. Table 4 summarizes a result of the gelation test for CA-MA dilute solutions in pyridine or DMSO, which were allowed to stand for two weeks at 20 °C before inspection of the fluidity. CA-$MA_{0.04}$ gelated at concentrations of ≥0.5 wt % in pyridine and of ≥2.0 wt % in DMSO, and CA-$MA_{0.09}$ gelated already at 0.5 wt % in both solvents. However, CA-$MA_{0.59}$ did not gelate at 0.5 wt % in solutions with any of pyridine and DMSO, notwithstanding that this CA-MA contains the largest amount of mercapto groups in the present CA-derivative series. This observation may be ascribed to a serious decrease in the molecular weight of CA-$MA_{0.59}$ due to acid decomposition (see Table 3). It is therefore concluded that CA-MA has a good capability for gelation even at such a lower mercaptoacetylated state as $DS_{SH} < 0.05$, but an excessive fall in the molecular weight depresses the capability.

Table 2. Preparation Conditions of CA-MA and wCA-MA Samples and DS Evaluation by ^{1}H NMR after Their Propionylation

sample code	starting material	reaction time/h	MAA in feed[a]	DS_{Ac}	DS_{SH}	MS_{MA}	DS_{Pr}
CA-$MA_{0.00}$	CA 1	0.5	12	2.11	0.00	0.01	0.91
CA-$MA_{0.04}$	CA 1	0.5	24	2.12	0.04	0.04	1.00
CA-$MA_{0.09}$	CA 1	2	24	2.01	0.09	0.11	0.86
CA-$MA_{0.15}$	CA 1	4	24	2.05	0.15	0.15	0.96
CA-$MA_{0.18}$	CA 1	8	24	2.03	0.18	0.23	1.10
CA-$MA_{0.24}$	CA 1	12	24	1.97	0.24	0.24	1.07
CA-$MA_{0.30}$	CA 1	14	24	1.62	0.30	0.37	1.35
CA-$MA_{0.36}$	CA 1	16	24	1.80	0.36	0.43	1.33
CA-$MA_{0.59}$	CA 1	24	24	1.35	0.59	0.71	1.66
CA-$MA_{0.19}$	CA 2	12	24	2.12	0.19	0.25	0.96
CA-$MA_{0.23}$	CA 2	18	24	1.96	0.23	0.29	1.07
wCA-$MA_{0.04}$	wCA	8	18	0.69	0.04	0.05	2.35

[a] Represented by the molar ratio to an anhydroglucose unit of CA.

Table 3. M_n, M_w, M_w/M_n, and DP_w of CA, wCA, CA-MA, and wCA-MA Samples, Estimated by GPC after Propionylation

sample code	$M_n/10^4$	$M_w/10^4$	M_w/M_n	DP_w
CA 1	7.52	19.1	2.54	632
CA 2	7.52	26.2	3.48	881
wCA	4.80	16.9	3.52	524
CA-$MA_{0.00}$	6.63	15.0	2.26	496
CA-$MA_{0.04}$	6.65	14.5	2.18	471
CA-$MA_{0.09}$	6.46	14.3	2.21	473
CA-$MA_{0.15}$	6.83	14.6	2.14	468
CA-$MA_{0.18}$	6.34	14.6	2.30	448
CA-$MA_{0.24}$	5.52	14.1	2.55	438
CA-$MA_{0.30}$	4.90	12.7	2.59	381
CA-$MA_{0.36}$	5.64	13.0	2.30	378
CA-$MA_{0.59}$	4.22	10.3	2.44	283
CA-$MA_{0.19}$	5.81	15.1	2.60	467
CA-$MA_{0.23}$	5.67	15.6	2.75	479
wCA-$MA_{0.04}$	5.48	16.5	3.01	506

For aqueous solutions of wCA-MA, the oxidation was carried out with bubbling of O_2 gas at 20 °C. Thereby wCA-$MA_{0.04}$ formed a hydrogel at 1.0 wt % and higher concentrations in a few days. Thus wCA-MA also has an adequate capability for gelation in the completely aqueous system at a relatively low value of $DS_{SH} = 0.04$.

We attempted to repeat the sol–gel transition of CA-MA in three cycles of redox treatments in order to confirm retention of its gelation ability. The cycle consisted of the following procedures at ambient temperature: oxidation in DMSO, solation with 50% AMaq for a less than 1 h period, and thorough reduction in 50% ME/DMI for 48 h, the latter two steps being followed by reprecipitation in methanol (see Experimental Section). As a consequence, it was found that 12 h was required for attainment of the first gel state and the gelating time was almost unchanged in the subsequent cycles. On the other hand, the wCA-MA sample was subjected to the sol–gel transition cycle at 20 °C twice: it was dissolved in water, oxidized with bubbling of O_2 gas, and reduced with ME (directly added onto the gel) over a period of 24 h. After reprecipitation in THF, the reduced sample was reused for the second cycle. As a result, it took ~48 h to achieve the first gelated state, while 480 h was required for the second gelation. This deceleration of gelation is possibly due to slight diminution of the originally lower DS_{SH}.

To see the influence of repetition of the sol–gel transition cycle for CA-MA and wCA-MA on the molecular compositions, the multiredoxed samples stated above, CA-MA-**o3r3** and wCA-MA-**o2r2**, were propionylated and their DS and MS were determined by ^{1}H NMR analysis. Table 5 shows the result of the quantification. DS_{Ac} was found to remain unchanged in all the samples tested, even in wCA-MA redoxed in the aqueous medium. Contrarily, DS_{SH} and MS_{MA} decreased to some extent, suggesting that the ester side chains dangling a mercapto group, involved actually in the redox reaction are prone to be eliminated from the backbone by the treatments. Corresponding to this, CA-MA should lose the capability of cross-linking gradually with increasing redox cycles, which was perceivable for particularly lower-mercaptoacetylated samples. However, CA-MA of a comparatively high DS_{SH} (e.g., CA-$MA_{0.30}$) can be supposed to maintain the cross-linking gelation ability even after a few tens of repetitions of the redox cycle, because the decreasing rate of DS_{SH} was about 0.01 a cycle and CA-$MA_{0.04}$ firmly showed the gelation behavior at ~3 wt % in DMSO in the standard test.

The success of the repeated redox reactions in solution was also verified by Raman spectroscopy for selected samples of CA-MA, each collected in a powder form at the respective junctures after oxidation and reduction treatments. To make an additional remark, the CA-MA powder obtained just after the

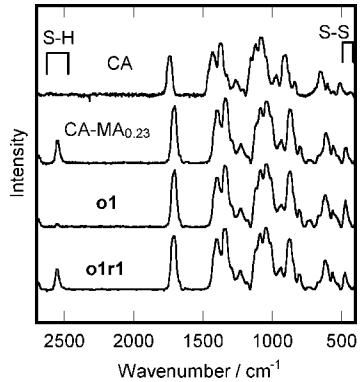

Figure 3. Raman spectra of CA, CA-$MA_{0.23}$, and redox-treated CA-$MA_{0.23}$ samples.

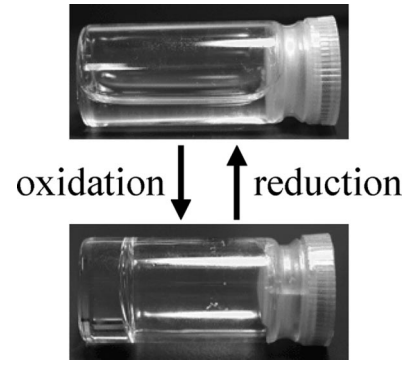

Figure 4. Visual appearance of a sol–gel transition of CA-$MA_{0.23}$, observed with DMSO as solvent and oxidant and with ME as reductant.

Table 4. Result of a Gelation Test for CA-MA Solutions That Were Allowed to Stand for Two Weeks at 20 °C before Visual Inspection of the Fluidity

		DS_{SH} of CA-MA[a]						
conc (wt %)	solvent	0.00	0.04	0.09	0.15	0.18	0.36	0.59
0.5	DMSO	×	×	○	○	○	○	×
0.5	pyridine	×	○	○	○	○	○	×
1.0	DMSO	×	×	○	○	○	○	○
1.0	pyridine	×	○	○	○	○	○	○
2.0	DMSO	×	○	○	○	○	○	○
2.0	pyridine	×	○	○	○	○	○	○

[a] See Table 3 regarding the molecular weight data. Symbols: ○, gelled; ×, could not gelate.

Table 5. DS and MS Data for CA-$MA_{0.23}$, CA-$MA_{0.30}$, wCA-$MA_{0.04}$, and Their Redox-Treated Samples, Estimated by ^1H NMR after Propionylation

sample code	DS_{Ac}	DS_{SH}	MS_{MA}	DS_{Pr}
CA-$MA_{0.23}$	1.96	0.23	0.29	1.07
CA-$MA_{0.23}$-**o3r3**	1.96	0.19	0.23	0.98
CA-$MA_{0.30}$	1.62	0.30	0.37	1.35
CA-$MA_{0.30}$-**o3r3**	1.62	0.27	0.30	1.34
wCA-$MA_{0.04}$	0.69	0.04	0.05	2.35
wCA-$MA_{0.04}$-**o2r2**	0.69	0.02	0.04	2.37

treatment with 50% AMaq preceded by oxidation in DMSO, imparted quite a feeble SH signal; this implies that the CA-MA was still in an immaturely reduced state.

Depth Scanning Raman Spectroscopic Characterization for CA-MA Films. To estimate the extent of prevalence of the redox reactions into the inside of CA-MA samples in film form, Raman spectra of as-cast CA-MA films and their redox-treated ones were measured by a depth scanning microscopic technique at five positions of $Z = 0$, 10, 20, 40, and 60 μm in depth from the surface of the respective films 120 μm thick. As a typical examination, 20% DMSOaq was used to oxidize CA-$MA_{0.23}$ at 60 °C for 24 h, and 10% MEaq, 10% AMaq, or 10% AM/DMIaq was used at 30 °C to reduce it. A 24 h treatment for the reduction was repeated until an increment of the SH peak intensity at 2575 cm^{-1} (I_{SH}) stopped at any altitude of $Z =$ 0–60 μm in the Raman measurement. The time period required for the utmost reduction of the oxidized CA-$MA_{0.23}$ was as follows: 504 h with 10% MEaq, 96 h with 10% AMaq, and 96 h with 10% AM/DMIaq.

Figure 5 illustrates the dependence of the peak intensity I_{SH} on the Raman scanning depth for films of as-cast CA-$MA_{0.23}$, CA-$MA_{0.23}$-**o1**, and three different CA-$MA_{0.23}$-**o1r1** samples, the latter three being reduced with 10% MEaq, 10% AMaq, and 10% AM/DMIaq for 504, 96, and 96 h, respectively, at 30 °C. In this figure, the intensity for the original cast CA-$MA_{0.23}$ is normalized as unity and relative values of I_{SH} are plotted for the post-treated samples. The data reveals that almost complete reduction throughout the inside of the film was accomplished by using 10% MEaq as the reductant. In contrast, the reduction with 10% AMaq was incomplete, the degree being lower at every position than that in the case using 10% MEaq. The degree of reduction with 10% AM/DMIaq was comparable to that with 10% AMaq at $Z \geq 20$ μm and, at the surface, nearly equal to that with 10% MEaq.

As is already commented in relation to the sol–gel transition of redoxed CA-MA, aqueous AM has a reducing power inherently stronger than that of ME, but the actual effectiveness and/or efficiency of reduction may be much affected by the compatibility of the reductants with the polymer substrate concerned. In the above Raman result, this is well reflected by the difference in the depth profile of I_{SH} between the 10% MEaq-treated CA-MA film and the 10% AMaq-treated one;

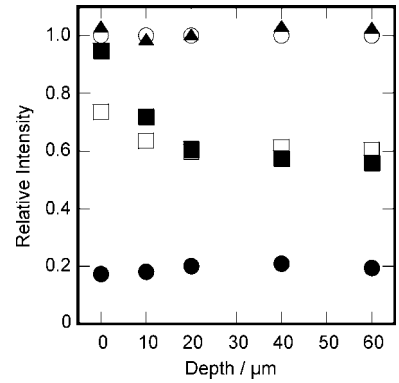

Figure 5. Relative intensity I_{SH} of a Raman peak at 2575 cm^{-1} associated with the SH group, estimated at different positions in depth for a CA-$MA_{0.23}$ cast film (120 μm thick) and its redox-treated samples: ○, as-cast CA-$MA_{0.23}$; ●, CA-$MA_{0.23}$-**o1** oxidized with 20% DMSOaq; ▲, CA-$MA_{0.23}$-**o1r1** reduced with 10% MEaq; □, CA-$MA_{0.23}$-**o1r1** reduced with 10% AMaq; ■, CA-$MA_{0.23}$-**o1r1** reduced with 10% AM/DMIaq.

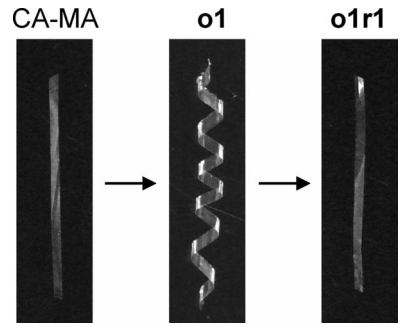

Figure 6. Example of observation of the shape memory-recovery behavior for a CA-$MA_{0.23}$ film ca. 6 μm thick.

there would be a good extent of compatibility in the former contact due to a stronger affinity of ME for CA-MA, contrary to the latter incompatible contact. To improve the reducing effect of 10% AMaq for CA-MA films, it was combined with DMI as a permeation mediator. As expected, the combination 10% AM/DMIaq displayed a higher reducing activity compared with 10% AMaq, at least to a depth of less than 20 μm from the film surface. Although 10% AM/DMIaq was still inferior to 10% MEaq in the perfection of reduction in the inside of the film sample, the time period required to saturate the reduction was considerably shorter with the combination, ca. a fifth of the period in the 10% MEaq-application. For earlier convenience, therefore, 10% AM/DMIaq may be available to reduce thinner films of several micrometers in thickness.

Shape Memory-Recovery Function. A shape memory-recovery function was tested for CA-$MA_{0.23}$ films 5–10 μm thick. Figure 6 demonstrates an example of the result. A long narrow slip of film was coiled around a slender glass rod at

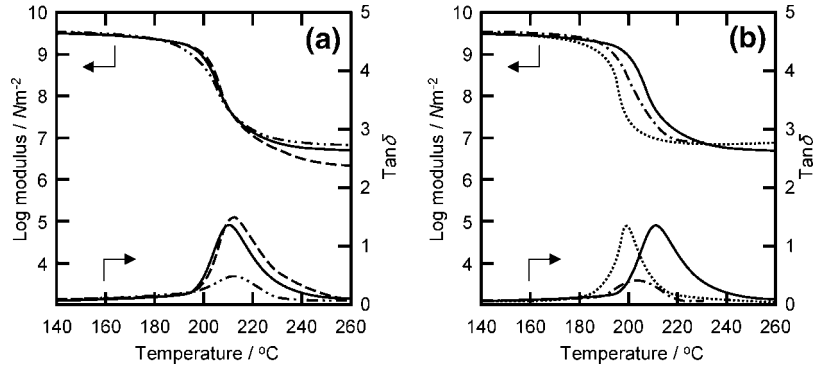

Figure 7. Temperature dependence of the dynamic storage modulus (E') and loss tangent (tan δ) for a CA-MA$_{0.23}$ cast film and its redox-treated samples: (a) data for as-cast CA-MA$_{0.23}$ (···), **o1** (-·-·-·), and **o1r1** (——); (b) data for **r1** (---), **o1r1** (——), and **o2r1** (-···-···-). See text for comparative discussion.

oxidized in 20% DMSOaq at 60 °C for 24 h with restraint of the formation. As shown in the figure, the oxidized film (**o1**) memorized the curly shape. After that, the film was reduced in 10% AM/DMIaq without restraint at 30 °C for 96 h. The reduction allowed the curled film to recover the original tabular shape. The redox cycle was repeated three times, and the film showed a good reversibility of the shape memory and recovery in the cyclic treatments.

Estimation of Cross-Linking Effect on Thermal and Viscoelastic Properties. As has been proved above, the CA-MA samples prepared were invested with a shape memory-recovery function. Undoubtedly, this function is owed to the occurrence and annihilation of the cross-linkage in which the mercapto groups participate. Next, the as-cast films and the redox-treated ones were examined by DSC and DMA for evaluation of the cross-linking effect on the thermal and viscoelastic properties.

Figure 7a shows the temperature dependence of the dynamic storage modulus E' and loss tangent tan δ for films of CA-MA$_{0.23}$ as-cast, CA-MA$_{0.23}$-**o1** oxidized with 20% DMSOaq, and CA-MA$_{0.23}$-**o1r1** reduced with 10% MEaq. The E' vs temperature curves of the respective samples exhibited a sharp drop in a temperature range of ca. 185–210 °C, which can be associated with their glass transition. However, the midpoint as well as the onset position of the E' drop shifted to the higher temperature side in the order of the redox treatments. Correspondingly, the peak top of tan δ also moved to higher temperature positions. Somewhat strangely, the principal dispersion of the reduced sample **o1r1** did not go back to the temperature position of the corresponding signal observed for the original untreated film. This may be interpreted as due to an effect of the annealing (i.e., thermal aging) and/or a chemical effect such as a trace of residual cross-linking or the deesterification of side chains leading to deplasticization of the CA-MA, each exerted on the sample by the redox treatments including drying.

A result of DSC measurements conducted for the CA-MA$_{0.23}$ as-cast film and its redox-treated samples is illustrated in Figure 8. The untreated cast film showed a clear baseline shift reflecting the glass transition in the thermogram and the midpoint T_g was evaluated as 194.5 °C; this value was almost equivalent to a T_g data (194.1 °C) for as-synthesized CA-MA$_{0.23}$ (powder). The oxidized sample **o1** exhibited no sharp T_g signal, which was also the case for the second run; the stiffening caused by effective intermolecular cross-linking is probably responsible for the indiscernible T_g behavior. In this connection, it should be noted that the **o1** sample gave a considerably lower tan δ peak with the maximum value less than 0.5 in the DMA

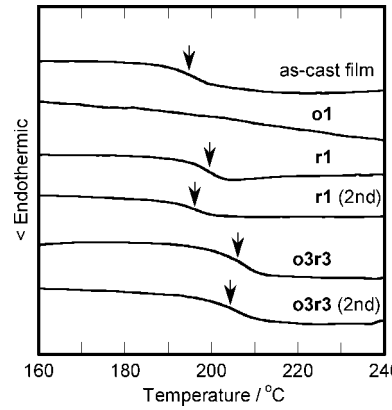

Figure 8. DSC thermograms of a CA-MA$_{0.23}$ as-cast film and its redox-treated samples. Arrows indicate a T_g position taken as the midpoint of the discontinuity in heat flow.

experiment (see Figure 7a). Figure 8 includes a thermogram measured for a CA-MA$_{0.23}$ film (**r1**) subjected solely to the reduction process with 10% MEaq after casting. The T_g was estimated to be 199.1 °C (first run), higher than that for the untreated film. In qualitative accordance with this, as shown in Figure 7b, a major, dynamic mechanical dispersion of the **r1** sample was centered at a higher temperature position, compared with the corresponding signal of the untreated film. The E' and tan δ data of the reduced sample rather resemble the respective ones of the **o1r1** sample. In the second DSC scan for the **r1** sample, however, we obtained T_g= 195.6 °C approaching the T_g of the untreated sample, possibly as a result of cancelation of the thermal history given in the reduction process.

When the cast CA-MA$_{0.23}$ film was treated in the redox cycle three times (**o3r3**), the T_g elevation became more prominent, as can be seen in Figure 8. The T_g of the **o3r3** sample was estimated to be 206.0 °C in the first heating and 204.1 °C in the second heating, both values being appreciably higher than 194.1 °C as an original T_g before the redox treatments. Therefore, in interpretation of the T_g shifting behavior, it seems reasonable to assume that a chemical effect following some change in the structure of CA-MA molecules could be predominant over the physical effect of thermal annealing. In DMA analysis for the **o3r3** film, it was also observed that the tan δ peak moved to the higher temperature side by about 10 °C relative to the corresponding location for the **r1** or **o1r1** sample. However, a CA-MA$_{0.23}$-**o2r1** film, being in the ultimately oxidized state, provided a smaller tan δ signal centering at nearly the same temperature position as that detected for the **o1r1** sample (see Figure 7b), and a similar positional relation was

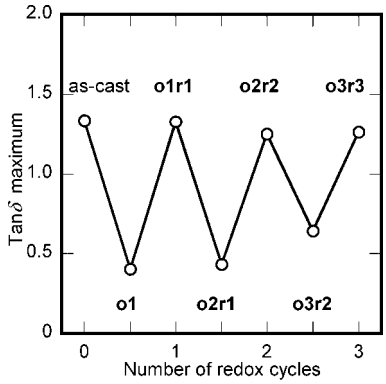

Figure 9. Values of the tan δ maximum observed for film samples of CA-$MA_{0.23}$, plotted as a function of the number of redox cycles.

found between the two data for **o3r2** and **o2r2** samples. These observations suggest that the major chemical factor contributing to the elevations of T_g and tan δ peak temperature would occur in the reduction treatment rather than in the oxidation. It is quite plausible that an ester hydrolysis of the side chains of CA-MA would proceed in the repeated, long-term reduction process in the aqueous medium, where the demercaptoacetylation is taken to precede the deacetylation, judging from the result in the sol–gel transition system (Table 5). To assess the degree of deesterification for CA-MAs multiredoxed in film form, we tried to propionylate the samples; however, this kind of films did not dissolve in pyridine, probably due to a certain extent of agglomeration or sintering as a result of the procedures of casting, redoxing, and drying. The CA-$MA_{0.23}$-**o3r3** film hardly swelled even in a reducing and dissolvent mixture of 50% ME/DMI. Thus, we could not make the ^{1}H NMR measurement. Instead, we carried out the depth scanning Raman measurement for the **o3r3** film and found that the relative intensity I_{SH} never recovered to unity but assumed values ranging from 0.85 (Z = 60 μm) to 0.87 (Z = 0 μm), supporting occurrence of the demercaptoacetylation in the repeated redox cycles.

In Figure 7, there appears a large difference in magnitude of the tan δ peak between the data obtained after oxidation and that after reduction, as we just referred to the matter in the above discussion. A plot of the respective maximum values of tan δ for the CA-$MA_{0.23}$ cast film and its posttreated samples is made in Figure 9 as a function of the number of redox cycles. We can see the tan δ magnitude repeating a decline(<1) and a good recovery (>1), respectively, following the oxidation and reduction. This alternating behavior reflects well a reversibility of the viscoelastic property of the cellulose derivative, which is comparatively elastic ($E'' < E'$) due to formation of the S–S cross-linking on oxidation and conversely becomes more viscous ($E'' > E'$) after the cleavage on reduction, when the polymer material is viewed in the glass transition temperature region. However, particularly the response of tan δ suppression on oxidation tends to weaken in the falling extent when the redox treatments are repeated more than two times, attributable to the progressive elimination of mercaptoacetyl groups.

Finally we give further attention to the DMA result shown for CA-$MA_{0.23}$ in Figure 7; there, the degree of lowering of E' in the glass transition region observed for the oxidized samples **o1** and **o2r1**was comparable to the corresponding E'-drop for the ultimately reduced samples such as **o1r1** and **o2r2**, in spite of the noticeable difference in the tan δ signal. It follows, therefore, that the density of the cross-linking points produced by the oxidation may be essentially low. Even if a kind of chain-segmental clusters would be formed due to local concentration of the cross-links, the clustering domain size should be within a few nanometer scale and the distance between the clusters should be large enough to permit an adequate mobility of the main-chains in the glass transition temperature region.

Conclusions

A series of SH-containing cellulose ester, CA-MA, was prepared by esterification of cellulose acetate (CA) with mercaptoacetic acid (MAA) in a homogeneous reaction system with a solvent 1,3-dimethyl-2-imidazolidinone (DMI). Particularly water-soluble CA-MA (wCA-MA) samples were synthesized via mercaptoacetylation of water-soluble CA obtained by acid hydrolysis of cellulose triacetate. The degrees of ester substitution (DSs) of the derivatives were evaluated successfully by ^{1}H NMR measurements after propionylation. DS_{SH} associated with the side chains possessing a mercapto end-group was an index characterizing the redox activity of the CA derivatives.

It was demonstrated that solutions of CA-MA (DS_{SH} = 0.04–0.59) showed a sol–gel transition by adequate redox treatments with dimethyl sulfoxide (DMSO) as solvent and oxidant and with 2-mercaptoethanol (ME) and/or ammonium mercaptoacetic acid (AM) as reductant. Similar sol–gel transition behavior was confirmed for aqueous solutions of wCA-MA (DS_{SH} = 0.04) by treatments with O_2 bubbling for oxidation and with ME for reduction. Repetition of the sol–gel transition for the respective mercaptoacetylated samples gave rise to a diminution in DS_{SH} as well as that in a molar substitution of MAA (MS_{MA}). However, the cross-linking gelation ability of CA-MA appeared to be effective even after a few tens of redox treatments, if the original $DS_{SH} \geq$ ca. 0.25, because a critical DS_{SH} value required for the gelation was quite low ($<$0.05).

Redox treatments for the CA-MA products were also carried out in film form by an immersion method with an aqueous DMSO solution (20 wt %) for oxidation and with an aqueous ME or AM solution (10 wt %) for reduction. The redox state (–SH or –SS–) of the mercapto groups of CA-MA could be monitored by Raman spectra measurements. Especially, the confocal depth scanning technique revealed the degree of penetration of the redox reagents into the interior of the film specimen. Owing to the difference between ME and AM in their affinity with the CA-MA substrate, the aqueous ME solution was preferable as a reducing reagent to accomplish the widespread reduction throughout the inside of the film sample, but a mixed solution of AM and DMI was available for faster reduction of thinner films or of the surface region in thicker films. In this context, it was visually demonstrated that solution-cast CA-MA films exhibited a shape memory-recovery function synchronously with the redox treatments.

Thermal and viscoelastic properties of CA-MA cast films and redox-treated ones were examined by DSC and DMA measurements for evaluation of the cross-linking effect. A derivative of DS_{SH} = 0.23 was mainly employed as the representative sample, which was oxidized with aqueous DMSO (20 wt %) and reduced with aqueous ME (10 wt %). Alternately declining and recovering behavior of the loss tan δ peak in the glass transition temperature (T_g) region was observed by following the repeated redox treatments of the CA-MA sample, reflecting well a reversible variation in the viscoelasticity due to the S–S cross-linkage formation on oxidation and its cleavage on reduction. However, thermal annealing and deesterification of side chains, both exerted on the CA-MA sample during the redox cycles, were liable to shift the T_g to the higher temperature side. The demercaptoacetylation occurring in the reductio

process was possibly the more effective factor. As a result of this elimination of mercaptoacetyl groups, the ability of shape memory-recovery of the CA-MA film decayed progressively with repetition of the redox treatments; nevertheless, the practical function was maintainable even after several cycles.

In view of the above fruitful examples of characterization, the CA-MA series may be expected to be a promising functional cellulose derivative applicable to the fields of fibers and films as a shape memory-recovery material.

Acknowledgment. We acknowledge Professor T. Matsumoto and Dr. D. Tatsumi of Kyoto University for having afforded the microscopic Raman measurement facilities.

Abbreviations

AM, ammonium mercaptoacetic acid
10% AMaq, 10 wt % aqueous solution of AM
50% AMaq, 50 wt % aqueous solution of AM
10% AM/DMIaq, a mixture of AM:DMI:H_2O = 10:10:80 in weight
CA, cellulose acetate
CA-MA, cellulose acetate mercaptoacetate
CA-MA*x*, CA-MA of $DS_{SH} = x$ (DS_{SH}, DS of side chains having a mercapto terminal)
CA-MA*x*-o*M*r*N*, CA-MA*x* that is oxidized *M* times and reduced *N* times
DMA, dynamic mechanical analysis
DMI, 1,3-dimethyl-2-imidazolidinone
DMSO, dimethyl sulfoxide
20% DMSOaq, 20 wt % aqueous solution of DMSO
DS, degree of substitution
DSC, differential scanning calorimetry
MAA, mercaptoacetic acid
ME, 2-mercaptoethanol
10% MEaq, 10 wt % aqueous solution of ME
50% ME/DMI, a mixture of ME:DMI = 50:50 in weight
wCA, water-soluble cellulose acetate
wCA-MA, water-soluble cellulose acetate mercaptoacetate
wCA-MA*x*, wCA-MA of $DS_{SH} = x$
wCA-MA*x*-o*M*r*N*, wCA-MA*x* that is oxidized *M* times and reduced *N* times

Supporting Information Available. FT-IR spectra, elemental analysis, and T_g estimation for CA-MA. This material is available free of charge via the Internet at http://pubs.acs.org.

References and Notes

(1) Nishio, Y. *Adv. Polym. Sci.* **2006**, *205*, 97–151.
(2) Klemm, D.; Heublein, B.; Fink, H. -P.; Bohn, A. *Angew. Chem., Int. Ed.* **2005**, *44*, 3358–3393.
(3) Ray Chaudhuri, D. K.; Hermans, J. J. *J. Polym. Sci.* **1960**, *48*, 159–166.
(4) Gemeiner, P.; Zemek, J. *Collect. Czech. Chem. Commun.* **1981**, *46*, 1693–1700.
(5) Siqueira Petri, D. F.; Choi, S. W.; Beyer, H.; Schimmel, T.; Bruns, M.; Wenz, G. *Polymer* **1999**, *40*, 1593–1601.
(6) Aoki, N.; Fukushima, K.; Kurakata, H.; Sakamoto, M.; Furuhata, K. *React. Funct. Polym.* **1999**, *42*, 223–233.
(7) Breier, A.; Gemeiner, P.; Ziegelhöffer, A.; Turi Nagy, L.; Štofaníková, V, *Colloid Polym. Sci.* **1987**, *265*, 933–937.
(8) Bernkop-Schnürch, A.; Hornof, M.; Guggi, D. *Eur. J. Pharm. Biopharm.* **2004**, *57*, 9–17.
(9) Schwenker, R. F., Jr.; Lifland, L.; Pacsu, E. *Text. Res. J.* **1962**, *32*, 797–804.
(10) Schwenker, R. F., Jr.; Lifland, L. *Text. Res. J.* **1963**, *33*, 107–117.
(11) Tesoro, G. C.; Sello, S. B.; Willard, J. J. *J. Appl. Polym. Sci.* **1968**, *12*, 683–697.
(12) Sakamoto, M.; Takeda, J.; Yamada, Y.; Tonami, H. *J. Polym. Sci., Part A-1*. **1970**, *8*, 2139–2149.
(13) Komarek, R. J.; Gardner, R. M.; Buchanan, C. M.; Gedon, S. *J. Appl. Polym. Sci.* **1993**, *50*, 1739–1746.
(14) Shibata, T. In *The Recent Trends of Glycochemistry*; Kobayashi, K., Shoda, S., Eds.; CMC Publishing Co., Ltd.: Tokyo, 2005; pp 121–132.
(15) Miyamoto, T.; Sato, Y.; Shibata, T. *J. Polym. Sci., Polym. Chem. Ed.* **1985**, *23*, 1373–1381.
(16) Tezuka, Y.; Tsuchiya, Y. *Carbohydr. Res.* **1995**, *273*, 83–91.
(17) Hussain, M. A.; Liebert, T.; Heinze. T., *Macromol. Rapid Commun.* **2004**, *25*, 916–920.
(18) Wallace, T. J. *J. Am. Chem. Soc.* **1964**, *86*, 2018–2021.
(19) Atalla, R. H. *Appl. Polym. Symp.* **1976**, *28*, 659–669.
(20) Wiley, J. H.; Atalla, R. H. *Carbohydr. Res.* **1987**, *160*, 113–129.
(21) Fischer, S.; Schenzel, K.; Fischer, K.; Diepenbrock, W. *Macromol. Symp.* **2005**, *223*, 41–56.

BM7006828